

# Helicity asymmetries in double pion photoproduction on the proton

February 15, 2019

L. Roca

*Departamento de Física Teórica and IFIC, Centro Mixto Universidad de Valencia-CSIC  
Institutos de Investigación de Paterna, Apdo. correos 22085, 46071, Valencia, Spain*

## Abstract

Based on a prior model on double pion photoproduction on the proton, successfully tested in total cross sections and invariant mass distributions, we make a theoretical study of the angular dependence of helicity asymmetries from the interaction of circularly polarized photons with unpolarized protons. We show that this observable is sensitive to details of the internal mechanisms and, thus, represents a complementary test of the theoretical model.

## 1 Introduction

The photoproduction of two pions on nucleons at low and intermediate energies (up to  $E_\gamma \sim 1$  GeV) has been the subject of intense experimental [1–6] and theoretical [7–13] study. The works have been mainly motivated to understand the role of the many baryonic resonances involved in the process. The fact that there are three particles in the final state,  $N\pi\pi$ , gives way to different mechanisms in which baryonic resonances play an important role, and this has led to obtain useful information on some resonances not attainable with other reactions. Much of the work has been done in unpolarized observables, mostly total cross sections and invariant mass distributions. In particular, the work of [13], which is the one we will use along this work, is based on around 25 Feynman diagrams considering the coupling of photons to several baryonic resonances able to influence the energy region up to  $E_\gamma \sim 800$  MeV. The main advantage is the use of no free parameters. This model succeeded in reproducing total cross sections and invariant mass distributions for all the charge channels with a good accuracy, not only in nucleons but also in nuclei. Specially remarkable was the application of the model of [13] to the study of the photoproduction of two pions in nuclei [14]. It succeeded in describing the shift of strength in the double

pion invariant mass distribution towards the  $2m_\pi$  masses, due to the modification of the  $\sigma$ -meson mass in nuclear matter, where the  $\sigma$ -meson is dynamically generated as a  $\pi\pi$  rescattering in scalar-isoscalar channel. This prediction was confirmed by the experiment of [15]. Therefore, the model of [13] has widely proven his efficiency in reproducing and predicting unpolarized observables in the energy range from threshold up to  $E_\gamma \sim 800$  MeV. Nonetheless, a more demanding test to the model can be done by evaluating polarization observables, since it can be sensible to details of the model not visible when integrating over polarization degrees of freedom in the unpolarized observables. In this line, a test of the model of [13] was done in [16] when evaluating the spin 1/2 and 3/2 amplitudes and the contribution to the GDH sum rule of the double pion channel, in fair agreement with Mainz results [17, 18], and the evaluation of beam asymmetries under experimental study at GRAAL [5]. These observables are based on differences of total differential cross sections dependent on polarization, which provide a valuable information on the internal dynamics of the reaction. However, these observables still rely on integrated cross sections and no angular distributions are provided from where more information can be obtained.

The aim of the present work is to evaluate angular dependences of the cross section asymmetry  $\sigma^+ - \sigma^-$  for the absorption of circularly polarized photons by unpolarized protons. This observable is very sensitive to the internal mechanisms of the reaction and, therefore, can be a very useful test to impose constraints on the theoretical models. The work has been partly motivated by preliminary experimental results, for the  $\gamma p \rightarrow \pi^+ \pi^- p$  channel, with the CLAS detector at Jefferson Lab [19] which shows strong and not trivial angular dependences of this observable, and prospects of measurements at Mainz [20] for the  $\gamma p \rightarrow \pi^0 \pi^0 p$  channel.

## 2 Summary of the $\gamma p \rightarrow \pi\pi p$ model

In this section we briefly summarize the model of [8, 9, 13] for the double pion photoproduction on nucleons. This model is intended to reproduce the total cross sections and invariant mass distributions up to photon energies of  $E_\gamma \sim 800$  MeV. The model is based on a set of tree level diagrams, depicted in Fig. 1, for the  $\pi^+ \pi^-$  channel. For the  $\pi^0 \pi^0$  channel only the mechanisms  $e, f, g, h, k, l, m, o, p, q, r$  and  $u$  contribute. These Feynman diagrams involve pions,  $\rho$ -mesons, nucleons and nucleonic and  $\Delta$  resonances. The baryon resonances included in the model are:  $\Delta(1232)$  or  $P_{33}$  ( $J^\pi = 3/2^+$ ,  $I=3/2$ ),  $N^*(1440)$  or  $P_{11}$  ( $J^\pi = 1/2^+$ ,  $I=1/2$ ),  $N^*(1520)$  or  $D_{13}$  ( $J^\pi = 3/2^-$ ,  $I=1/2$ ) and  $\Delta(1700)$  or  $D_{33}$  ( $J^\pi = 3/2^-$ ,  $I=3/2$ ). The contribution of the  $N^*(1440)$  is small but it was included due to the important role played by that resonance in the  $\pi N \rightarrow \pi\pi N$  reaction and the fact that the excitation of the  $N^*(1440)$  peaks around 600 MeV photon energy in the  $\gamma N$  scattering. The  $N^*(1520)$  has a large coupling to the photons and is an important ingredient due to its interference with the dominant term of the process, the  $\gamma N \rightarrow \Delta\pi$  transition called the  $\Delta$ -Kroll-Ruderman ( $\Delta$ KR) contact term. (The  $\Delta$ KR term is not present in the  $\gamma p \rightarrow \pi^0 \pi^0 p$  channel). Several  $\rho$  and  $\Delta(1700)$  terms were included in the last version of the model [13] because of important interference effects. The consideration of the  $\rho$  terms was of crucial

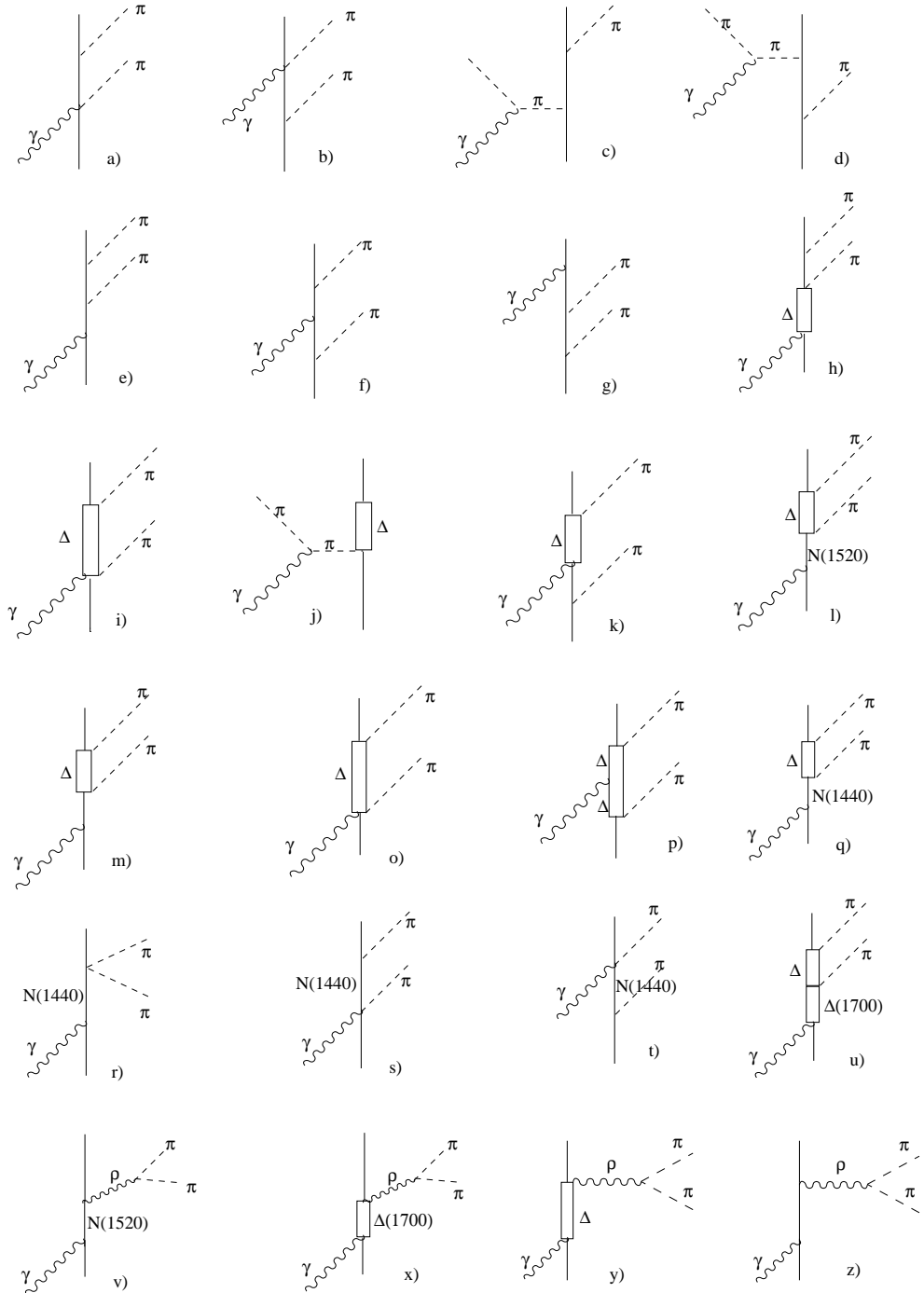


Figure 1: Feynman diagrams used in the model for  $\gamma p \rightarrow \pi^+ \pi^- p$ . Solid lines without labels are nucleons.  $\Delta$  means  $\Delta(1232)$ . For the  $\gamma p \rightarrow \pi^0 \pi^0 p$  channel only the  $e, f, g, h, k, l, m, o, p, q, r$  and  $u$  mechanisms contribute.

importance in the analysis of Ref. [21], when studying  $\rho$  meson photoproduction in nuclei. The  $y$ ) and  $z$ ) diagrams considering a  $\rho$  exchange were not considered in [13] since they give negligible contribution to the cross section in the energy region of concern. However they were considered in the work of [21] by completeness when considering  $\rho$  meson photoproduction and we also include them here since they can produce a non-negligible influence in the polarization asymmetry.

No other resonances were considered in the model since they cannot appreciably change the results in the energy range up to  $E_\gamma \sim 800$  MeV, because their widths are small and lie at too high energies, because the helicity amplitudes are small, because the decay width rates into  $\Delta\pi$  or  $\rho N$  are small or because a combination of various of these effects [13].

The diagrams u), v) and x) of Fig. 1 are the main modifications of [13] with respect to [9]. In the first work of [8] they included more than 50 diagrams for the  $\gamma p \rightarrow \pi^+ \pi^- p$  channel, but many of them were shown to be negligible at energies up to  $E_\gamma = 800$  MeV. The non-negligible contributions come from the diagrams of Fig. 1.

The amplitudes are evaluated from effective interaction Lagrangians which are shown in the Appendices of Ref. [13], using a non relativistic approximation exact up to order  $p/M_p$ , that is, removing terms of order  $(p/M_p)^2$  and higher.

It is important to stress that this model has no free parameters, in the sense that there is no parameter to be fitted to the experimental double pion photoproduction observable. All input needed is obtained uniquely from properties of resonances and their decays. Where there are doubts about relative signs of couplings, one resorts to quark models or chiral perturbation theory to fix them [22].

### 3 Photon helicity asymmetry

We will consider the absorption of circularly polarized photons by non-polarized protons. For real photons the polarization vectors of a circularly polarized photon can be expressed as:

$$\vec{\epsilon}^\pm = \frac{1}{\sqrt{2}}(\mp 1, -i, 0) \quad (1)$$

where  $\vec{\epsilon}^+$  or  $\vec{\epsilon}^-$  represent a right-handed or left-handed circularly polarized photon respectively.

The helicity asymmetry that we are going to consider in the present work can be defined as

$$A \equiv \frac{d\sigma^+ - d\sigma^-}{d\sigma^+ + d\sigma^-} \quad (2)$$

where  $d\sigma^{+(-)}$  is the differential cross section for the interaction of a right-handed (left-handed) circularly polarized photon with an unpolarized proton.

Three different frames have been commonly used in the literature to describe angular distributions in three body final state processes [23–25]. These frames are called *Gottfried-Jackson*, *helicity* and *Adair* systems, differing in the choice of the  $z'$  axis from which the azimuthal and polar angles are defined. The choice of a particular frame is of relevance

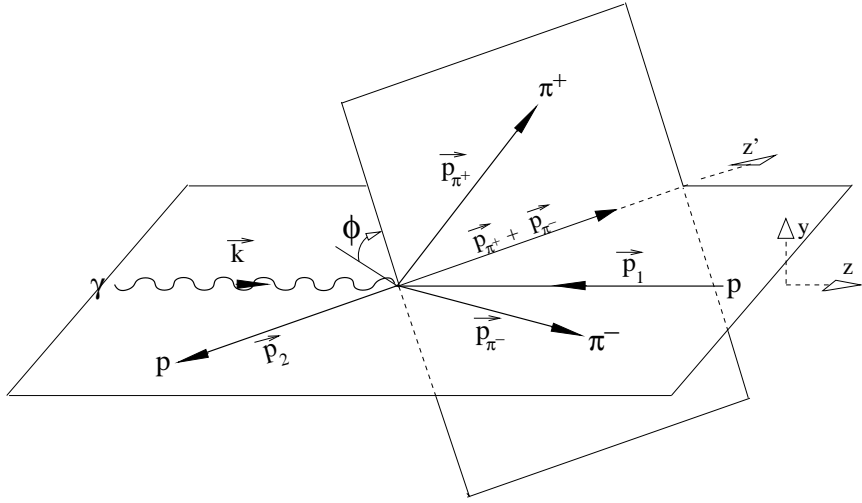


Figure 2: Angular and kinematics definition in the helicity frame.

when studying particular production processes, like vector-meson photoproduction, due to particular angular distributions for a certain spin of the intermediate meson. In the present work, in order to test all the possible mechanisms contributing to the  $\gamma p \rightarrow \pi^+ \pi^- p$  process, any of these frames is useful for our purposes. Therefore, in order to allow comparison with preliminary experimental results with the CLAS detector at Jefferson Lab [19], we will use the *helicity* frame, which is defined as having the  $z'$  axis in the direction of the sum of the momentum of both pions in the overall ( $\gamma p$ ) c.m. frame. The use of the other frames would produce similar qualitative results for the discussion done in the present work. In Fig. 2 the kinematics for the  $\gamma(k)p(p_1) \rightarrow \pi^+(p_{\pi^+})\pi^-(p_{\pi^-})p(p_2)$  reaction in this *helicity* frame is shown.

In the present work we will consider the  $\phi$  dependence of the  $A$  observable since it is very sensitive to the particular mechanisms involved in the reaction by different reasons. First, it is sensible to differences of cross sections,  $(\sigma^+ - \sigma^-)$ , and thus mechanisms which give small contribution to the total cross section can produce a sizeable contribution to the helicity asymmetry if the mechanisms are strongly helicity dependent. Second, it is very sensitive to interferences between the different diagrams of the model, as we explain in detail below.

Let us write the amplitude for the process as

$$T = \epsilon_\mu T^\mu. \quad (3)$$

In order to evaluate the cross sections one has to consider the squared  $T$ -matrix averaged over the initial spin of the proton, since we are considering non-polarized target, and summed over the spins of the final proton:

$$\sum_{s_i, s_f} \langle m_{s_i} | \epsilon_\mu T^\mu | m_{s_f} \rangle \langle m_{s_f} | \epsilon_\nu^* T^{\dagger \nu} | m_{s_i} \rangle = \text{Tr} \{ \epsilon_\mu T^\mu \epsilon_\nu^* T^{\dagger \nu} \}. \quad (4)$$

By using Coulomb gauge, where  $\epsilon_0 = 0$  and transversality,  $\epsilon_z = 0$ , with  $\hat{z}$  the direction of the photon momentum, Eq. (4) reads

$$Tr\{|\epsilon_x|^2 T_x T_x^\dagger + |\epsilon_y|^2 T_y T_y^\dagger + \epsilon_x \epsilon_y^* T_x T_y^\dagger + \epsilon_x^* \epsilon_y T_y T_x^\dagger\}. \quad (5)$$

Should we use linearly polarized photons ( $\vec{\epsilon} = (1, 0, 0)$  or  $(0, 1, 0)$ ), we would obtain for the numerator of Eq.(2) up to phase space integrals,  $Tr\{T_x T_x^\dagger - T_y T_y^\dagger\}$ <sup>1</sup> (which is roughly the *beam asymmetry*  $\Sigma$  already studied in [16]). If we use circularly polarized photons, the numerator of Eq.(2) goes as (up to phase space integrals):

$$d\sigma^+ - d\sigma^- \sim -2Tr\{i(T_x T_y^\dagger - T_y T_x^\dagger)\} = 4\mathcal{Im}\{Tr\{T_x T_y^\dagger\}\} = -2iTr\{(\vec{T} \times \vec{T}^\dagger)_z\} \quad (6)$$

where  $(\vec{T} \times \vec{T}^\dagger)_z$  means the component in the photon direction of the cross product of  $\vec{T}$  and  $\vec{T}^\dagger$ .

The amplitudes of the model provide  $\vec{T}$  which contains vectors proportional to  $p_{\pi^-}$ ,  $p_{\pi^+}$ ,  $\vec{k}$ , spin, crossed products of these vectors, etc. In order to interpret the final results it is useful to note that, since in Eq. (6) one is summing over nucleon spins, terms proportional to  $\vec{\sigma}$  in  $Tr\{\vec{T} \times \vec{T}^\dagger\}$  will vanish. Hence, for practical purposes, one could obtain the same result for Eq. (6) as with using the full amplitude, by taking an effective amplitude constructed only with momentum vectors. Hence, we can write

$$\vec{T}_{eff} = a_1 \vec{p}_{\pi^-} + a_2 \vec{p}_{\pi^+} + a_3 \vec{k} + a_4 (\vec{p}_{\pi^-} \times \vec{p}_{\pi^+}) + a_5 (\vec{p}_{\pi^-} \times \vec{k}) + a_6 (\vec{p}_{\pi^+} \times \vec{k}) \quad (7)$$

proportional to the identity matrix in the space of nucleon spin. The  $a_i$  coefficients are, in general, scalar complex functions including all the dynamics of the different mechanisms (propagators, momentum dependences of the vertices, etc). Furthermore, it is easy to show that for the purpose of evaluating the helicity asymmetry of concern in the present work it is enough to reduce Eq. (7) to

$$\vec{T}_{eff} = a \vec{p}_{\pi^-} + b \vec{p}_{\pi^+} \quad (8)$$

since combinations with the other terms of Eq. (7), when doing the cross product of Eq. (6), either vanish or reduce to something proportional to  $(\vec{p}_{\pi^-} \times \vec{p}_{\pi^+})_z$ , that is what one would obtain from Eq. (8). In fact, the general result for the numerator of the helicity asymmetry, by using Eqs. (6) and (8), reads, up to phase space integrations, as

$$d\sigma^+ - d\sigma^- \sim \mathcal{Im}(ab^*)(\vec{p}_{\pi^-} \times \vec{p}_{\pi^+})_z. \quad (9)$$

Let us discuss some important consequences that can be concluded from Eq. (9) on the sensitivity of the helicity asymmetry to the internal structure of the mechanisms and to the interferences between different diagrams. In some mechanisms it is allowed to have either

---

<sup>1</sup>In the nomenclature of "hadronic tensor",  $W^{\mu\nu}$ , and "structure functions" it would be  $\sim (W^{xx} - W^{yy}) = W_{TT}$ . (See, for instance, ref. [26]).

a  $\pi^+$  or a  $\pi^-$  in both the two external pion lines (we will call it type-I diagrams), while in other diagrams only one charge configuration is possible (type-II). (Type-II diagrams are  $a, b, c, d, e, f, g, h, k, p, s, t, v, x, y$  and  $z$  of Fig. 1 and type-I are the rest). For instance, in the  $\Delta KR$  term ( $i$  diagram of Fig. 1) it is possible to have a  $\pi^+$  in the  $\gamma N \Delta \pi$  vertex and a  $\pi^-$  in the  $\Delta N \pi$  vertex or vice-versa, while in the  $a$  diagram only the mechanism where the  $\pi^+$  in the  $\gamma N N \pi$  vertex and the  $\pi^-$  in the  $N N \pi$  vertex is possible.

If we take any individual diagram, by virtue of Eq. (6), the crossed product will necessarily vanish. Hence, associating diagrams to mechanisms, only the mechanisms that have two possible diagrams associated, i.e., those of type-I, could by themselves be nonzero. On the other hand, as seen in Eq. (9), one needs  $\mathcal{Im}(ab^*) \neq 0$  which means the coefficients  $a, b$  to be complex, and this is provided by the propagator structure of the diagrams. This is the reason why this observable is so sensitive to the internal mechanisms of the reaction. On the other hand, the  $(\vec{p}_{\pi^-} \times \vec{p}_{\pi^+})_z$  factor of Eq. (9) makes the numerator of  $A$  to be proportional to  $\sin \phi$ , therefore the difference from a simple  $\sin \phi$  dependence comes from the momentum dependence of the  $a$  and  $b$  coefficients of the amplitude. Thus, the angular dependence of the helicity asymmetry is strongly reflecting the internal structure of the various mechanisms.

On the other hand, when allowing the different mechanisms to interfere between them, they can produce factors  $ab^*$  with  $a \neq b$ . Thus, even if the individual mechanisms do not produce an asymmetry by themselves, they can produce a non-vanishing asymmetry when adding them coherently. This is why the interferences in the  $\phi$  dependence of the helicity asymmetry are so important. The angular dependence of the denominator of the helicity asymmetry,  $d\sigma^+ + d\sigma^-$  (that is proportional to the total cross section), does not modify qualitatively the previous discussion.

Let us illustrate the previous discussion with an example: let us consider the  $\Delta KR$  term ( $i$  diagram of Fig. 1). The amplitude for the process where the  $\pi^+$  is emitted before the  $\pi^-$  is given by [13]

$$\vec{T}_{\Delta KR} = \frac{1}{9} e \left( \frac{f^*}{m_\pi} \right)^2 G_\Delta(p_2 + p_{\pi^-}) F_\pi((p_{\pi^+} - k)^2) [2\vec{p}_{\pi^-} - i(\vec{\sigma} \times \vec{p}_{\pi^-})], \quad (10)$$

where  $f^* = 2.13$ ,  $G_\Delta$  is the  $\Delta(1232)$  propagator and  $F_\pi$  is a form factor. For the process where the  $\pi^-$  is emitted before the  $\pi^+$  the amplitude is obtained by exchanging  $p_{\pi^+} \leftrightarrow p_{\pi^-}$  and writing the appropriate isospin coefficients

$$\vec{T}_{\Delta KR} = -\frac{1}{3} e \left( \frac{f^*}{m_\pi} \right)^2 G_\Delta(p_2 + p_{\pi^+}) F_\pi((p_{\pi^-} - k)^2) [2\vec{p}_{\pi^+} - i(\vec{\sigma} \times \vec{p}_{\pi^+})]. \quad (11)$$

With these expressions for the amplitude, we have for the last term of Eq. (6)

$$Tr\{(\vec{T} \times \vec{T}^\dagger)_z\} = 20i \mathcal{Im}(\alpha\beta^*)(\vec{p}_{\pi^-} \times \vec{p}_{\pi^+})_z. \quad (12)$$

with  $\alpha = \frac{1}{9} e \left( \frac{f^*}{m_\pi} \right)^2 G_\Delta(p_2 + p_{\pi^-}) F_\pi((p_{\pi^+} - k)^2)$  and  $\beta = -\frac{1}{3} e \left( \frac{f^*}{m_\pi} \right)^2 G_\Delta(p_2 + p_{\pi^+}) F_\pi((p_{\pi^-} - k)^2)$ . This means that the  $\Delta KR$  mechanism (accounting for two Feynman diagrams) gives by itself a non-vanishing angular dependence of the helicity asymmetry thanks to the

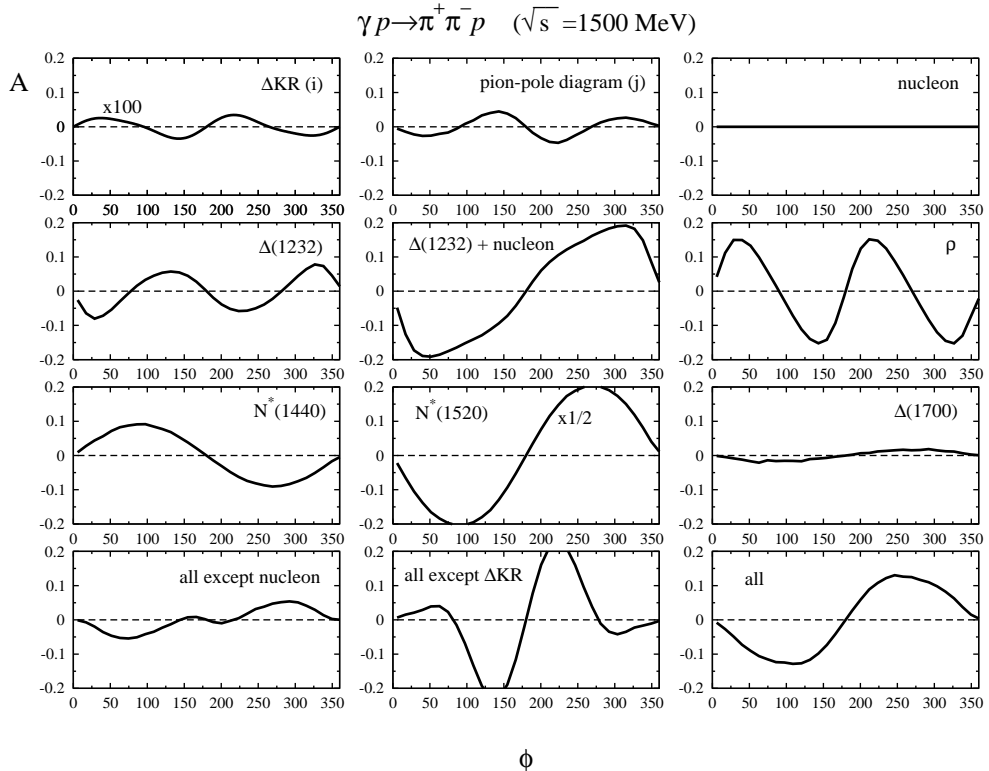


Figure 3: Angular ( $\phi$ ) distribution of the helicity asymmetry,  $A$ , for different contributions in the  $\gamma p \rightarrow \pi^+ \pi^- p$  channel for a  $\gamma p$  energy of  $\sqrt{s} = 1500$  MeV.

imaginary part in the  $\Delta$  propagator, and deviation from a simple  $\sin \phi$  dependence (as will be shown in the Results section) is due to the momentum dependence of the propagator and the form factor, (although this latter one is a smooth function).

The kind of reasoning presented in this section stresses the importance of small details of the theoretical models, making the  $\phi$  dependence of the helicity asymmetry a very useful and powerful tool to check the heart of the theoretical models. Therefore, even if the model succeeds to reproduce unpolarized observables (like total cross sections, invariant mass distributions, etc), it could fail to reproduce the kind of polarization observables studied in this work, simply because of small details.

## 4 Results

In Fig. 3 we show, for a given  $\gamma p$  energy of  $\sqrt{s} = 1500$  MeV ( $E_\gamma^{Lab} \simeq 730$  MeV), the  $\phi$  distribution of the helicity asymmetry,  $A$ , for different mechanisms contributing to the  $\gamma p \rightarrow \pi^+ \pi^- p$  process. From left to right and up to down the plots represent:  $\Delta$ KR term ( $i$  diagram of Fig. 1), pion pole term ( $j$  diagram), nucleon intermediate mechanisms (diagrams from  $a$  to  $g$ ),  $\Delta(1232)$  (diagrams  $h$  to  $k$  and  $m$  to  $p$ ),  $\rho$ -meson intermediate contribution (diagrams  $v$  to  $z$ ),  $N^*(1440)$  resonance (diagrams  $q$  to  $t$ ),  $N^*(1520)$  (diagrams

$l$  and  $v$ ),  $\Delta(1700)$  (diagrams  $u$  and  $x$ ), all the mechanisms except the nucleon intermediate diagrams, all the mechanisms except the  $\Delta$ KR term and, finally, the full model (all the diagrams). (The plots of the  $\Delta$ KR term alone and the  $N^*(1520)$  have been multiplied by 100 and 1/2 respectively to make the curves visible inside the represented scale). The fact that  $A(\phi) = -A(2\pi - \phi)$  is a necessary condition since the change  $\phi \rightarrow (2\pi - \phi)$  can be interpreted as a reflection of the  $\vec{p}_{\pi^+}\vec{p}_{\pi^-}$  plane with respect to the  $\vec{k}\vec{p}_2$  plane (see Fig. 2). This is equivalent to changing the sign of the  $y$  coordinate and, therefore, by looking at Eq. (1), to the exchange of the role right-handed $\leftrightarrow$ left-handed, what means  $A \rightarrow -A$ . The condition  $A(\phi) = -A(2\pi - \phi)$  implies that  $A$  can be expanded as

$$A(\phi) = \sum_{n=1}^{\infty} a_n \sin(n\phi), \text{ with } n = 1, 2, 3, 4, \dots \quad (13)$$

One can see in Fig. 3 the very strong dependence on the mechanisms considered and the crucial role of the interferences. For instance, even if the nucleon intermediate mechanisms give a vanishing contribution by themselves, the interference with the  $\Delta(1232)$  mechanisms produces strong changes in the distribution with respect to considering the  $\Delta(1232)$  terms alone. Another quantitative example of the important role of the interferences can be seen, for instance, by looking at the figures evaluated with all the mechanisms except the nucleons or except the  $\Delta$ KR term. For this latter case, despite the asymmetry for the  $\Delta$ KR being very small, it has an important influence in the full result. On the other hand, by comparing the "all except nucleon" with the "all" plot, one can see the dramatic influence of the nucleon intermediate mechanism in the angular distribution of the helicity asymmetry, despite these mechanisms contributing only around 10% to the total cross section.

In order to show the sensitivity to the energy of the angular distribution of the helicity asymmetry, we show in Fig. 4 the results with the full model for different energies. The experimental data, still preliminary, are obtained from Ref. [19], measured with the CLAS detector at Jefferson Lab. It is important to stress that these data are integrated over the full CLAS acceptance, while the theoretical model covers the full phase space. Thus, given the sensitivity of the observable to these details, one has to be cautious when making conclusions from this naive comparison. With this caveat, and after the remarks on the sensitivity of this observable to small details of the model, the comparison of the theoretical predictions of the present work and the data of [19] shown in Fig. 4 would be seen as an indication that the model contains the basic mechanisms. The strength of the theoretical results and experiment is similar, and this is not a trivial theoretical result given the large range of values found in Fig. 3 for different options of partial results of the model. The discrepancies found in the shape for the two lower energies are more worrisome, but in view of the preliminary character of the experimental data, and the fact that they are not  $4\pi$  integrated, it is probably too early to draw conclusions from there. We would like to note that the theoretical results reported here are similar in strength and shape as those reported in [19] as private communication, calculated with the model of [27]. In view of this, it is important that definitive data are provided and that direct calculations adapted to the acceptance of the experimental setup are carried out. This comparison should help

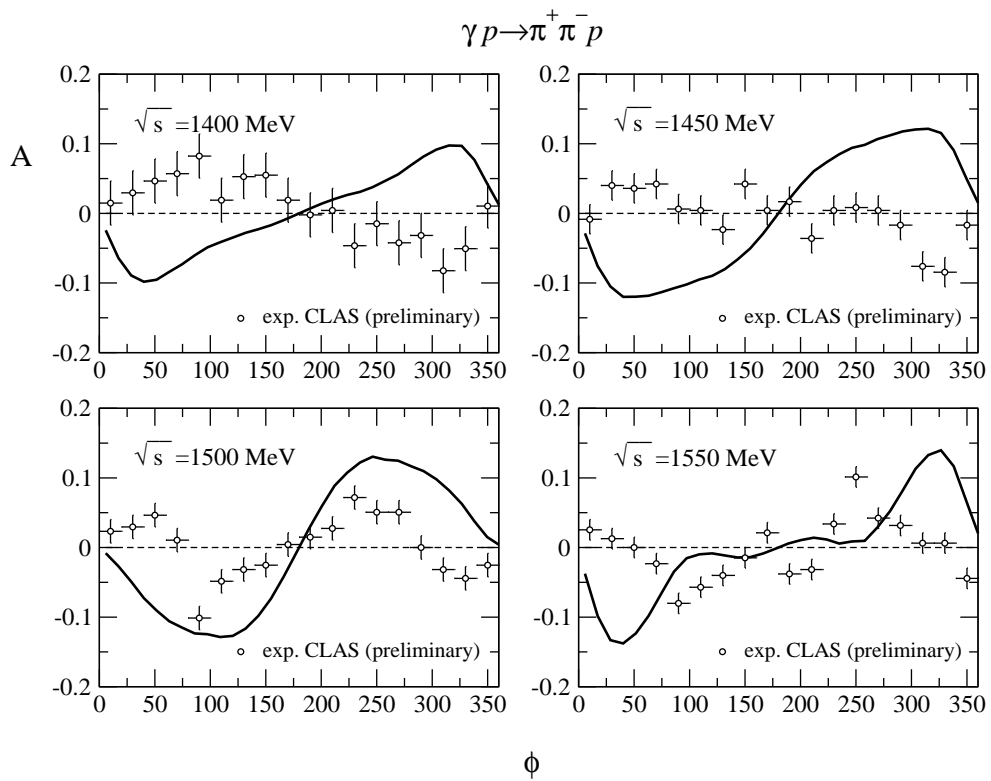


Figure 4: Angular distribution of the helicity asymmetry for different energies with the full model, for the  $\gamma p \rightarrow \pi^+ \pi^- p$  channel. Preliminary experimental results from [19]. (The data is integrated over the full CLAS acceptance while the theoretical calculations cover the full phase space).

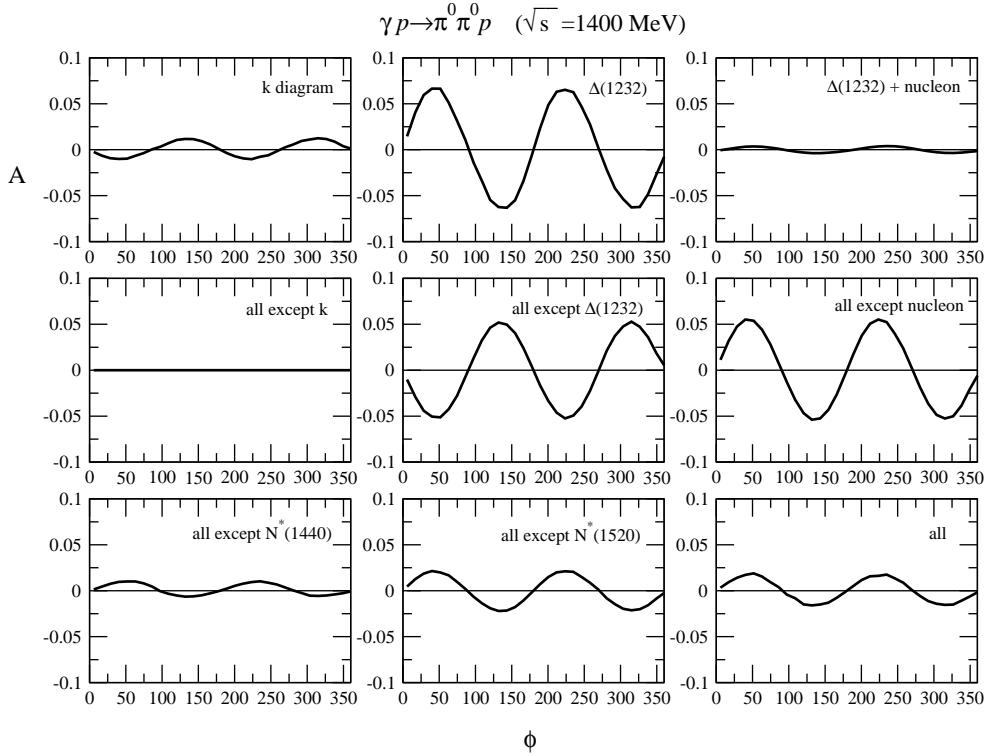


Figure 5: Angular ( $\phi$ ) distribution of the helicity asymmetry,  $A$ , for different contributions in the  $\gamma p \rightarrow \pi^0 \pi^0 p$  channel for a  $\gamma p$  energy of  $\sqrt{s} = 1400$  MeV.

in the future to fine tune the present models of double pion photoproduction.

Next we show the results for the  $\gamma p \rightarrow \pi^0 \pi^0 p$  channel, for which there are prospects to be measured at Mainz [20]. In Figs. 5 and 6 we show the contribution of different mechanisms, or combinations between them, for two different energies. In the  $\pi^0 \pi^0$  channel there are less mechanisms allowed than in the  $\pi^+ \pi^-$  case, like, for instance, the  $\Delta$ KR term (which gives the most important contribution in the  $\pi^+ \pi^-$  channel). From left to right and up to down the plots in Figs. 5 and 6 represent:  $k$  diagram (which is important in the total cross section [13]),  $\Delta(1232)$  (diagrams  $h, k, m, o$  and  $p$ ),  $\Delta(1232)$  plus nucleon terms, all the mechanisms except  $k$ , all except  $\Delta(1232)$ , all except nucleon, all except  $N^*(1440)$ , all except  $N^*(1520)$  and , finally, the full model.

In this channel, apart from the condition  $A(\phi) = -A(2\pi - \phi)$ , there is another extra condition which is  $A(\phi) = A(\phi + \pi)$ . This happens since the two  $\pi^0$  are identical particles and the observables cannot depend on permuting the two  $\pi^0$ , but the exchange of the two pions means the change  $\phi \rightarrow \phi + \pi$  (see Fig. 2). The conditions  $A(\phi) = -A(2\pi - \phi)$  and  $A(\phi) = A(\phi + \pi)$  imply that, in the series of Eq. (13) only the  $n =$ even terms are possible. That is why the angular dependence of the helicity asymmetry for the  $\pi^0 \pi^0$  channel manifests, essentially, a  $\sin(2\phi)$  shape. For this reason, the shape for this channel is less rich in variety of structures than in the  $\pi^+ \pi^-$  case, since the  $\sin(\phi)$ ,  $\sin(3\phi), \dots$  terms are

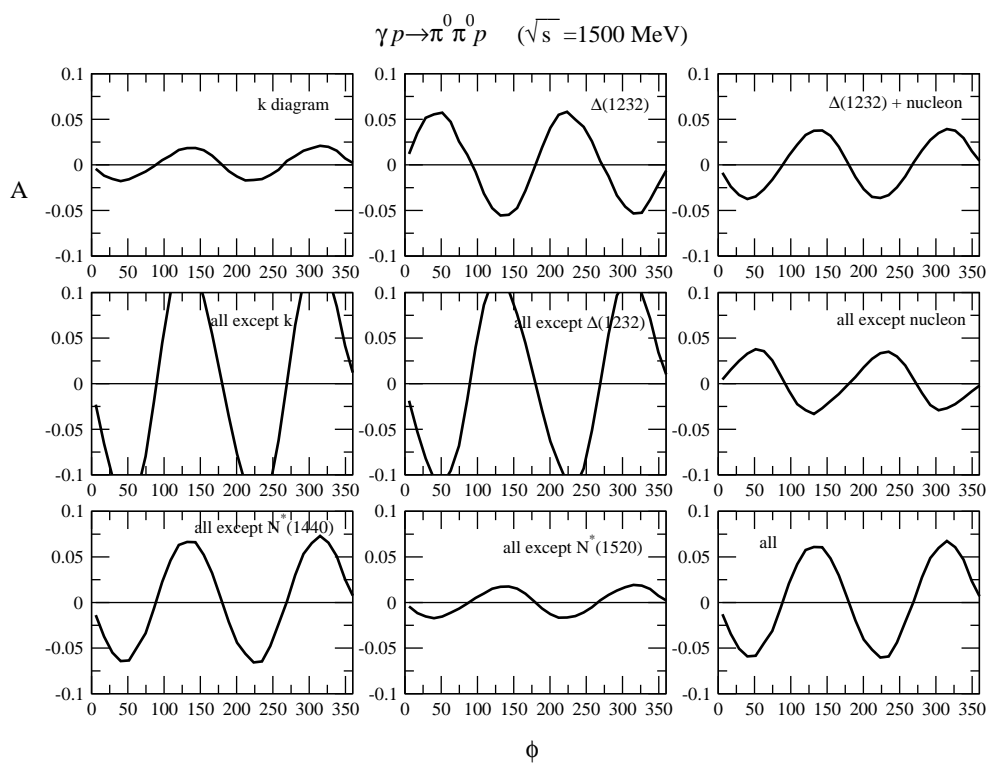


Figure 6: Same as Fig. 5 for  $\sqrt{s} = 1500$  MeV.

forbidden. Nonetheless, despite the plots in Figs. 5 and 6 manifesting mainly a  $\sin(2\phi)$  dependence, one can see there the important role of interferences in determining the strength and phase (sign) of the distributions, and the energy dependence of the effect. For instance, for  $\sqrt{s} = 1400$  MeV, despite the nucleon mechanisms giving a vanishing contribution by themselves (not shown in the figure), the interference with the  $\Delta(1232)$  mechanisms produces a very small asymmetry. Another example, quite spectacular, is the role of the  $k$  diagram since, in spite that by itself gives a similar distribution for both energies, the distribution removing it from the full model looks dramatically different in the two energies: in fact, at 1400 MeV, the angular distribution of the asymmetry is negligible if one removes the  $k$  mechanism from the full model, while at 1500 MeV the effect is very large. The  $N^*(1520)$  reduces the strength at 1500 MeV if it is removed from the full model, while no significant effect is visible at 1400 MeV. Therefore, in spite the  $\pi^0\pi^0$  channel having less richness in different shapes for the distribution, the large variation in the strength and sign stresses the importance of this observable in elucidating the mechanisms involved in the reaction.

The calculations done in the present work are just an example of the type of studies that one can make, in the sense that other energies, angles or kinematical cuts can be implemented, but it serves as an example of the strong dependence on the internal mechanisms and interferences that is obtained from this kind of polarization experiments.

## 5 Conclusions

We have made calculations of angular distributions of helicity asymmetries in  $\gamma p \rightarrow \pi^+\pi^-p$  and  $\gamma p \rightarrow \pi^0\pi^0p$  for the interaction of circularly polarized photons with unpolarized protons. We have used a well tested theoretical model successfully applied in the evaluation of several unpolarized observables. The study of polarization observables of the kind of those discussed in the present work, can serve to challenge the theoretical models when more demanding refinement of the details can be crucial. We have shown the strong dependence of the shape and strength of the calculations on the internal mechanisms and interferences among different contributions to the process. We have shown that, in spite that some mechanisms do not give structure by themselves, they can be crucial to produce the final result due to subtle interferences with other mechanisms. Furthermore, mechanisms which give a small contribution in unpolarized observables, like total cross sections, can be of strong relevance in the contribution to the difference between the polarization cross sections. All these facts stress the conclusion that these observables are extremely sensitive to the internal details of the models, providing strong challenges to the theoretical models.

Further experimental results would be of importance to discriminate between models but being aware that sizeable discrepancies between theoretical and experimental results can be due to small details which are irrelevant when applying the model to the evaluation of unpolarized observables.

## 6 Acknowledgments

I acknowledge support from the Ministerio de Educación, Cultura y Deporte. I thank fruitful discussions with E. Oset and M. J. Vicente Vacas. This work is partly supported by DGICYT contract number BFM2003-00856, and the E.U. EURIDICE network contract no. HPRN-CT-2002-00311.

## References

- [1] A. Braghieri *et al.*, Phys. Lett. B **363** (1995) 46.
- [2] A. Zabrodin *et al.*, Phys. Rev. C **55** (1997) 1617.
- [3] F. Harter *et al.*, Phys. Lett. B **401** (1997) 229.
- [4] M. Wolf *et al.*, Eur. Phys. J. A **9** (2000) 5.
- [5] Y. Assafiri *et al.*, Phys. Rev. Lett. **90** (2003) 222001.
- [6] M. Kotulla *et al.*, Phys. Lett. B **578** (2004) 63.
- [7] L. Y. Murphy and J. M. Laget, DAPNIA-SPHN-96-10
- [8] J. A. Gomez Tejedor and E. Oset, Nucl. Phys. A **571** (1994) 667.
- [9] J. A. Gomez Tejedor and E. Oset, Nucl. Phys. A **600** (1996) 413.
- [10] K. Ochi, M. Hirata and T. Takaki, Phys. Rev. C **56** (1997) 1472.
- [11] M. Hirata, K. Ochi and T. Takaki, Phys. Rev. Lett. **80** (1998) 5068.
- [12] M. Ripani *et al.*, Nucl. Phys. A **672** (2000) 220.
- [13] J. C. Nacher, E. Oset, M. J. Vicente and L. Roca, Nucl. Phys. A **695** (2001) 295.
- [14] L. Roca, E. Oset and M. J. Vicente Vacas, Phys. Lett. B **541** (2002) 77.
- [15] J. G. Messchendorp *et al.*, Phys. Rev. Lett. **89** (2002) 222302.
- [16] J. C. Nacher and E. Oset, Nucl. Phys. A **697** (2002) 372.
- [17] M. Lang [A2 and GDH Collaborations], *Prepared for Meson 2002: 7th International Workshop on Meson Production, Properties and Interaction, Cracow, Poland, 24-28 May 2002*
- [18] J. Ahrens *et al.* [GDH and A2 Collaborations], Phys. Lett. B **551** (2003) 49.
- [19] S. Strauch [the CLAS Collaboration], arXiv:nucl-ex/0407008.

- [20] R. Beck, *Private communication*.
- [21] E. Oset, L. Roca, M. J. Vicente Vacas and J. C. Nacher, arXiv:nucl-th/0112033. *Contribution to International Workshop on Chiral Fluctuations in Hadronic Matter, Orsay, France, 26-28 Sep 2001*
- [22] J. A. Gomez Tejedor, F. Cano and E. Oset, Phys. Lett. B **379** (1996) 39.
- [23] [Aachen-Berlin-Bonn-Hamburg-Hidelberg-Munich Collaboration], Phys. Rev. **175** (1968) 1669.
- [24] K. Schilling, P. Seyboth and G. E. Wolf, Nucl. Phys. B **15** (1970) 397 [Erratum-ibid. B **18** (1970) 332].
- [25] J. Ballam *et al.*, Phys. Rev. D **5** (1972) 545.
- [26] S. Boffi, C. Giusti, F.D. Pacati, and M. Radici, *Electromagnetic Response of Atomic Nuclei* (Clarendon Press, Oxford, 1996).
- [27] V. I. Mokeev *et al.*, Phys. Atomic Nucl. **66**, 1282 (2003); V. I. Mokeev *et al.*, Phys. Atomic Nucl. **64**, 1292 (2001).